On the use of knee functional calibration to determine the medio-lateral axis of the femur in gait analysis: Comparison with EOS biplanar radiographs as reference

Christophe Sauret, PhD[a,*], Hélène Pillet, PhD[a], Wafa Skalli, PhD[a], Morgan Sangeux, PhD[b,c]

[a] *Institut de Biomécanique Humaine Georges Charpak, Arts et Métiers ParisTech, 151 boulevard de l'Hôpital, F-75013 Paris, France*
[b] *Hugh Williamson Gait Analysis Laboratory, The Royal Children's Hospital, 50 Flemington Road, Parkville Victoria, 3052 Melbourne, Australia*
[c] *The Murdoch Children's Research Institute, Melbourne, Australia*

Keywords:
Biplanar radiographs
Femur
Functional calibration
Gait analysis
Knee
Medio-lateral axis

A B S T R A C T

Accurate calibration of the medio-lateral axis of the femur is crucial for clinical decision making based on gait analysis. This study proposes a protocol utilizing biplanar radiographs to provide a reference medio-lateral axis based on the anatomy of the femur. The biplanar radiographs allowed 3D modelling of the bones of the lower limbs and the markers used for motion capture, in the standing posture. A comprehensive analysis was performed and results from biplanar radiographs were reliable for 3D marker localization (±0.35 mm) and for 3D localization of the anatomical landmarks (±1 mm), leading to a precision of 1° for the orientation of the condylar axis of the femur and a 95% confidence interval of ±3° after registration with motion capture data. The anatomical condylar axis was compared to a conventional, marker-based, axis and three functional calibration techniques (axis transformation, geometric axis fit and DynaKAD). Results for the conventional method show an average difference with the condylar axis of 15° (SD: 6°). Results indicate DynaKAD functional axis was the closest to the anatomical condylar axis, mean: 1° (SD: 5°) when applied to passive knee flexion movement. However, the range of the results exceeded 15° for all methods. Hence, the use of biplanar radiographs, or an alternative imaging technique, may be required to locate the medio-lateral axis of the femur reliably prior to clinical decision making for femur derotational osteotomies.

1. Introduction

Gait analysis quantifies kinematics and kinetics of the lower limbs during walking to inform surgical decision making [1]. For example, it is crucial to interpret hip rotation kinematics in relation to the anatomy of the femur (e.g. femoral neck anteversion) prior to deciding upon femur derotation osteotomy [2]. However, hip rotation kinematics is among the least repeatable output of gait analysis [3]. Hip rotation is calculated as the angle between the medio-lateral axes of the femur and the pelvis in the transverse plane of the femur [4]. The medio-lateral axis of the femur is considered the culprit for the lack of reliability of hip rotation kinematics [5].

Conventional gait models determine the medio-lateral axis from markers placed over the lateral and medial epicondyles, or from the position of a knee alignment device [6]. These models are affected by marker placement errors and authors have proposed alternative functional methods [7]. Functional methods use the movement of the knee joint to determine an optimal flexion-extension axis (FLEXaxis) embedded in the femur coordinate system [7,8]. In gait analysis, the cross-product of this axis with the longitudinal axis (defined from knee to hip joint centres) determines the anterior-posterior axis. Then, the cross product of the anterior-posterior axis and the longitudinal axis determines the medio-lateral axis. Therefore, both FLEXaxis and medio-lateral axes are in the frontal plane of the femur but only the medio-lateral axis is constrained to be perpendicular to the longitudinal axis. These functional methods were validated *in silico* [7] and sometimes by means of mechanical devices [9,10]. The validation *in vivo* has focused on intra and inter examiner reliability [5,11,12].

New 3D modelling from low dose biplanar radiographs [13] allows the simultaneous acquisition of the position of bone-

* Corresponding author.
E-mail addresses: christophe.sauret@ensam.eu (C. Sauret), helene.pillet@ensam.eu (H. Pillet), wafa.skalli@ensam.eu (W. Skalli), morgan.sangeux@rch.org.au (M. Sangeux).

http://dx.doi.org/10.1016/j.gaitpost.2016.09.008

embedded joint centres and axes as well as markers used for motion analysis *in vivo*, with the subjects in a neutral standing posture [14,15]. The aims of this study were (1) to propose and evaluate a benchmark to locate the medio-lateral axis of the femur based on biplanar radiographs (BPR) and (2) to compare a range of conventional and functional methods based on skin-mounted markers against the BPR medio-lateral axis.

2. Materials and method

Following approval by the relevant ethics committee, 13 healthy volunteers (8 males and 5 females) participated to this study. On average, the subjects were 33 years (SD: 14, range: 22–60), height was 1.74 m (SD: 0.09 m, range: 1.55–1.92 m), body mass was 73 kg (SD: 12 kg, range: 54–91 kg) and Body Mass Index (BMI) was 23.9 kg/m^2 (SD: 3.8 kg/m^2, range: 16.8–29.4 kg/m^2). The protocol for the study has been described previously [14]. The subjects were equipped with 14 mm skin markers (Fig. 1a) tracked at 100 Hz with 8 T10 Vicon cameras (Vicon, Oxford Metrics, UK). Standing static calibration acquisition was performed, followed by knee functional calibration and walking trials. Low-dose biplanar radiographs (EOS® system, EOS imaging, France) were acquired immediately after, without removing the markers.

2.1. Proposal and evaluation of a benchmark to locate the medio-lateral axis of the femur

Three-dimensional shape models of the femurs were deformed and fitted to the frontal and sagittal radiographs [16] (Fig. 1b). We defined the centre of the femoral head (FH) and the centres of the medial (MPC) and lateral (LPC) posterior aspect of the condyles (Fig. 1c) by least square fitting spheres to the node of the mesh in the corresponding anatomical regions. The knee joint centre (KJC) was defined as the mid-point between MPC and LPC. The medio-lateral axis was defined by the transcondylar axis (TCA), the axis passing through MPC and LPC (Fig. 1c) [17]. The skin markers positions in EOS were obtained from 14 mm spheres positioned by matching their contours with that of the markers in the radiographs (Fig. 1b).

The joint centres and TCA axis was assessed on the right femurs of six subjects three times by two skilled examiners. The reproducibly variance (S_{Ri}^2, [18]) which include intra- and between-assessors repeatability variances was calculated as follows:

$$S_{Ri}^2 = S_{ri}^2 + S_{Li}^2 \quad (1)$$

where S_{ri}^2 is the mean of the assessor variances, and S_{Li}^2 is the variance of the mean results obtained by each assessor, for a particular ith subject. The global reproducibility estimate (S_R) was calculated as:

$$S_R = \sqrt{\frac{\sum_{i=1}^{n} S_{Ri}^2}{n}} \quad (2)$$

where n is the number of subjects.

Reliability of the marker positions from BPR was assessed based on the entire marker sets for four subjects, assessed three times by four examiners. We calculated the rigid transformation between the thigh marker sets determined from BPR and motion capture systems through least square fit [19]. Reliability was calculated as the root mean square distance (RMSD) between the two marker sets after registration.

The combined uncertainty was quantified from 100 000 Monte-Carlo simulations per subject. Random isotropic Gaussian noise was added to the BPR and motion capture data. Noise magnitude was defined from the estimates obtained above for BPR data and by a standard deviation of 1 mm for the motion capture data [20]. This procedure was performed for all subjects and the overall reliability was calculated using Eq. (2) with S_{Ri} corresponding to the standard deviation of the simulations for the ith subject, and $n = 13$.

2.2. Evaluation of conventional and functional methods to define the medio-lateral axis

The conventional gait method used two markers located over the medial and lateral epicondyles of the knee. The epicondyles were palpated and the markers positioned by an orthopedic surgeon. We implemented three functional methods to determine the knee axis: the axis transformation technique (ATT, [7]), the geometrical technique [21] and DynaKAD, which finds the axis that minimises the variance in the frontal plane kinematics at the knee [8]. The functional methods were applied to two movements: five

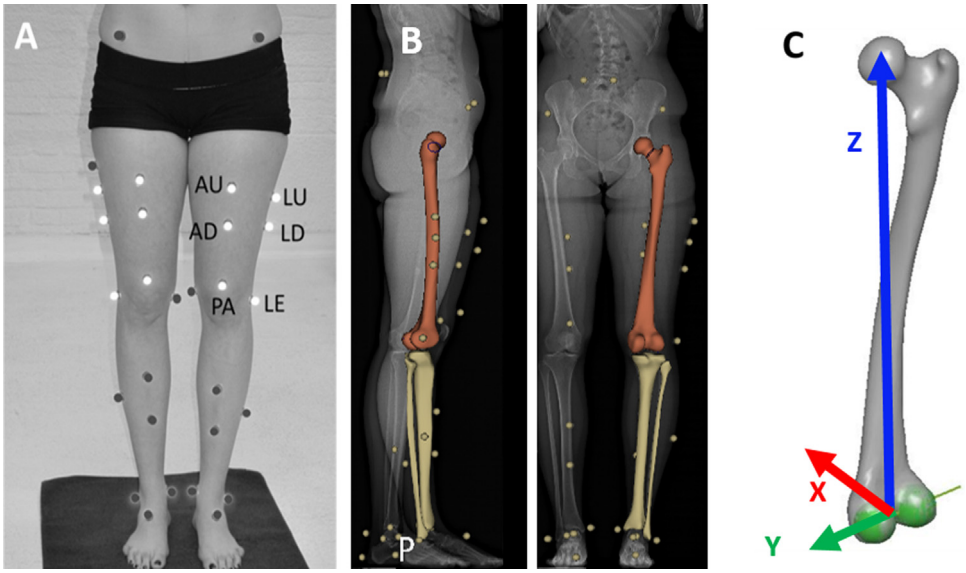

Fig. 1. A) Front view of the subject equipped with reflective markers. White markers are those used in this study to perform the registration whereas grey markers were not present during the biplanar radiographs acquisition or not used here. B) Lateral and coronal radiographs for the right limb with superimposed bony reconstructions and registered markers. C) Subject-specific reconstruction of the right femur with spheres fitted on posterior aspects of the condyles and transcondylar axis.

knee flexion-extensions (open kinematic chain) and three walking strides. Trials were captured with subjects walking continuously at 5 km/h on a treadmill for approximately one minute. Foot contact and foot off events were selected visually for one stride and auto-correlated in Nexus (Vicon, Oxford Metrics Group, UK). Three strides in the middle of the trial were processed for the functional calibration. The five knee flexion-extensions were performed assisted or unassisted to simulate the effect of lack of selective motor control in pathological populations [15]. For each frame, the transformation matrix between the static and dynamic poses of the thigh and shank marker sets were obtained from least square fit [19].

The location of the anatomical transepicondylar axis (BPR-based TEA) was also determined, as the 3D shape model of the femur contained regions that correspond to the medial and lateral epicondyles of the femur.

The reference anatomical coordinate system of the femur was constructed from the BPR-based data registered in the motion capture environment (FH, KJC and TCA, Fig. 1). The primary axis (Z, inferior-superior, perpendicular to the transverse plane of the femur) was specified by the vector from KJC to FH. The X-axis (posterior-anterior, perpendicular to the frontal plane of the femur) was calculated from the cross product between the primary axis and TCA as the secondary axis. The Y-axis (perpendicular to the sagittal plane of the femur) was defined as the cross product between Z- and X- axes. Similar femur coordinate systems were constructed using the same primary axis but different secondary axes, from functional calibrations or marker-based instead of TCA.

The angular difference between the Y-axes of the different femur coordinate systems was calculated to compare the different medio-lateral axes. Repeated measure ANOVA and post-hoc Tukey's pairwise comparisons were performed to rank and group the methods according to the angular difference with BPR-based TCA.

Hip and knee kinematics were calculated during walking to investigate the impact on kinematics. The pelvis coordinate system was defined using 4 markers taped over the left, and right, anterior, and posterior, superior iliac spines (L/R A/P SI). The origin was defined from the mid-point between LASI and RASI, and the medio-lateral axis (primary, Y-) from RASI to LASI. The superior-inferior axis (Z-, pointing up) was perpendicular to the transverse plane containing LASI, RASI and the mid-point between LPSI and RPSI. The anterior-posterior axis (X-, pointing forward) resulting from the cross-product of Y- and Z-. The tibia coordinate system was defined using two additional markers taped over the medial and lateral malleoli (MED and ANK respectively). The longitudinal axis (primary, Z-) was defined from the mid-point between the ANK and MED markers to the KJC. The anterior-posterior axis (X-, pointing forward) was perpendicular to the plane containing KJC, and the ANK and MED markers. The medio-lateral axis (Y-) resulted from the cross-product of Z- and X-. Hip and knee angles were calculated following ISB recommendations [22] adapted to the coordinate systems defined above. All processing was performed in Matlab® (The Mathworks, USA) and statistical analysis in Minitab (Minitab Inc., USA).

3. Results

3.1. Reliability of BPR-based data and registration with motion capture system

The reproducibility estimate (S_R) for the BPR-based parameters ranged between 1.0 and 1.4 mm for the location of FH, MPC and LPC (Table 1) and was 0.8 mm for KJC and 1.0° for TCA. The reproducibility estimate for marker location was similar for all markers and about 0.35 mm. Mean differences in marker positions after least square fitting between BPR-based and motion capture based markers showed RMSD of 2.2 mm (range: 0.7–4.4 mm). No correlation was found between RMSD and subject height ($r = 0.23$; $p = 0.24$), body weight ($r = 0.27$; $p = 0.16$) nor body mass index ($r = 0.39$, $p = 0.04$). The overall uncertainty of the protocol, estimated from the Monte-Carlo simulations, was 1.5 mm for the joint centre location and 1.5° for axis orientation. The 95% confidence intervals were therefore ±3 mm for KJC and ±3° for TCA.

Table 1
Reliability of specific points and knee joint centre following each direction of the femur reference frame and the norm. Reliability is expressed through the reproducibility estimate (S_R).

	Unit	X-axis	Y-axis	Z-axis	Norm
Femoral head	mm	1.2	0.6	0.5	1.4
Lateral posterior condyle	mm	0.7	0.9	0.4	1.2
Medial posterior condyle	mm	0.7	0.5	0.5	1.0

3.2. Evaluation of conventional and various functional methods to define the medio-lateral axis of the femur

Fig. 2 presents the results for the comparison of methods to define the medio-lateral axis of the femur in the motion capture environment. The mean difference between the BPR-based TCA and TEA was mean (SD): 5.7° (1.4°). All the methods used in gait analysis provided medio-lateral axes more external than TCA. The DynaKAD method provided axes that were closest to TCA with mean angular differences of 9° (5.4°), 1° (5.1°), 8° (4.8°) for the active FE, passive FE and walking calibration movements, respectively. Results for the geometrical method were further external compared to TCA and with larger standard deviation than DynaKAD: 14° (6.8°), 4° (7.5°), 15° (11.8°) for the active FE, passive FE and walking calibration movements, respectively. Results for the ATT transformation technique produced standard deviation values of a similar magnitude to DynaKAD but more external mean angular differences of 14°(6.5°), 10°(5.5°), 12°(6.0°) for the active FE, passive FE and walking calibration movements, respectively. For all methods, the active FE and walking movements resulted in larger deviation than for the passive FE movement. Results for the marker based method were external with respect to TCA with average difference of 15° (5.9°).

The orientation of the femur medio-lateral axis had a direct effect on the hip rotation kinematics, and some effect on the frontal plane knee kinematics, during gait. Fig. 3 illustrates these effects when the functional calibration methods were applied to the passive FE movement. On average during the gait cycle, hip rotation was about 10° internal for the BPR-based model (black) whereas all other models were more external, except for DynaKAD. The orientation of the femur medio-lateral axis had no effect on the knee kinematics in the sagittal plane since both FH and KJC were defined from the same BPR-based data.

4. Discussion

In gait analysis, the medio-lateral axis of the femur contributes to the definition of hip rotation kinematics, a key variable to inform decision making about femur derotational osteotomy. We aimed to propose a reference method to locate the medio-lateral axis of the femur based on bi-planar radiographs (BPR) and to evaluate a range of conventional and functional methods.

We estimated the reliability of BPR-based knee parameters (FH, KJC and TCA), marker localization and the registration between BPR and motion capture systems. Reliability of 3D marker

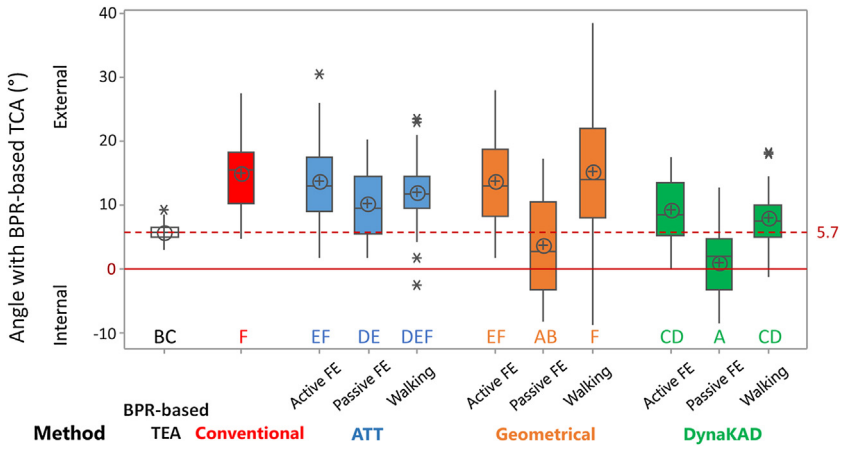

Fig. 2. Boxplot of the angular difference of the different medio-lateral axes of the femur with respect to the EOS-based transcondylar axis (TCA). The boxes are represented with a different colour for each method: red for marker based, blue for ATT/SARA functional, orange for geometrical functional, and green for DynaKAD functional. For the functional methods, three boxes are plotted corresponding to the three possible calibration movements: active flexion-extension (Active FE), passive flexion-extension (Passive FE) and Walking. The mean for each box is represented with a cross in a circle, asterisks represent outliers. The letters at the bottom of each box represent the grouping results from the post-hoc Tukey's ranking from A, the closest to the BPR-based TCA, to F, the furthest. Groups who share letters were not significantly ($\alpha < 0.05$) different from each other. (For interpretation of the references to colour in this figure legend, the reader is referred to the web version of this article.)

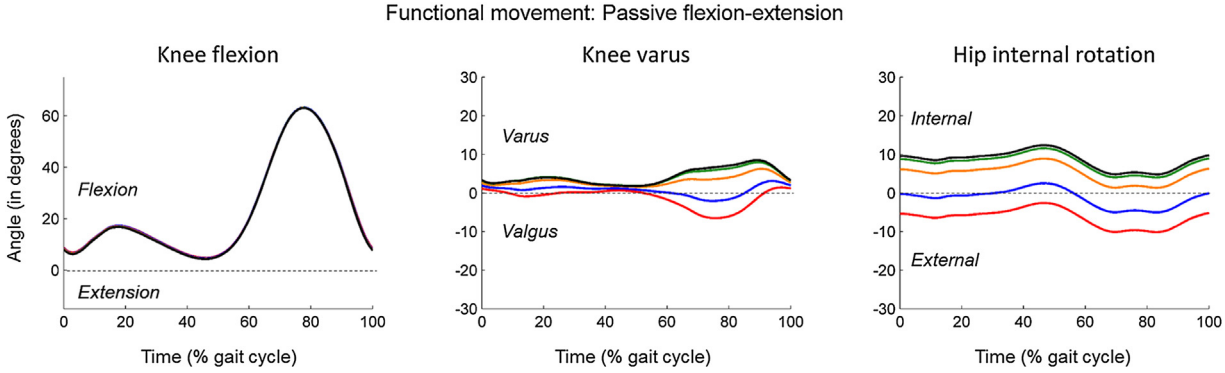

Fig. 3. Effect of the femur medio-lateral axis definition on hip and knee kinematics for each functional method associated with the passive knee flexion/extension movement. The variability in kinematics is represented by shaded bands representing the one standard deviation at each time instant. The marker and EOS-based TCA induced kinematics were also represented for visual comparisons. The reference knee kinematics corresponding to the EOS-based TCA is shown in black, kinematics from the marker based method is shown in red, kinematics from the geometrical functional method is shown in orange, kinematics from the ATT/SARA functional method is shown in blue and the kinematics from the DynaKAD functional method is shown in green. The foot contact and foot off events were determined visually (rather than from forceplate data) which led to a gait cycle slightly shifted. (For interpretation of the references to colour in this figure legend, the reader is referred to the web version of this article.)

localization from bi-planar radiographs ($S_R = 0.35$ mm) appears satisfactory compared to other sources of error in human movement analysis [20,23,24] and confirms previous results [14]. The reliability of BPR-based knee parameters was satisfactory with reproducibility around 1 mm for KJC and 1° for TCA. The registration of the thigh marker clusters between the two static standing poses led to RMSD of 2 mm on average. Monte-Carlo simulations revealed the 95% confidence interval was ±3 mm for KJC location and ±3° for TCA. These results demonstrate the suitability of a biplanar radiographic system such as the EOS system with the associated 3D reconstruction methods to serve as a reference method to locate the medio-lateral axis of the femur.

The BPR-based transcondylar axis (TCA) was compared with a range of conventional and functional calibration methods. The conventional method used markers over the medial and lateral epicondyles of the femur and showed a difference with TCA of about 15° external. Such a difference may not be attributed to the angular difference between the TEA and TCA axes since differences found in the literature ranged between 2.7° and 6.9° [25–27]. We found a difference between the BPR-based TEA and TCA of 5.7° external, in agreement with the literature. The angular difference between marker-based TEA and TCA is likely to be due to marker misplacement. A limitation of our study is that the person who palpated the epicondyles did not perform marker placement as part of routine clinical practice. However, the intra-observer reliability (6°) in our study was in agreement with previous findings [28].

Functional calibration methods use the knee axis as a proxy for the medio-lateral axis of the femur. We tested three algorithms, the geometrical method, the Axis Transformation Technique (ATT) and DynaKAD. The methods were tested on three different movements, 5 repetitions of a passive (assisted) or active (self-performed) open kinematic chain knee flexion-extension and 3 walking strides. The DynaKAD method provided the closest axis to the BPR-based TCA. The geometrical functional method was close to the BPR-based TCA when used in combination with passive flexion-extension but with more variable results (SD: 7.5°) than for DynaKAD (SD: 5.1°). The ATT functional method was more external (average mean: 12°, average SD: 5.5°) than the reference BPR-based TCA. Overall, our results were in agreement with a recent study using 3D freehand ultrasound (rather than BPR) to locate the TCA axis [29].

The ATT and geometrical functional methods model the knee joint as a single fixed axis hinge joint. However, the knee axis has been shown to move, both in location and in orientation, during knee flexion [30,31]. The motion of the knee may be better modelled as a two hinges joint: one for flexion-extension and one for internal/external rotation. Such a model of the knee defines flexion-extension as the movement around the medio-lateral axis of the femur and internal/external rotation as the movement around the longitudinal axis of the tibia. It corresponds well with the Cardan angles used for the knee joint: first, flexion-extension around the Y-axis of the femur coordinate system, then, varus/valgus around the anterior-posterior axis of the intermediate coordinate system and last, internal/external rotation around the longitudinal axis of the tibia [32]. The DynaKAD method finds the orientation of the Y-axis of the femur which minimises the variance in knee varus/valgus. This approach is equivalent to using the two hinges model described above and may explain why the axis provided by DynaKAD was found to be the closest to the BPR-based TCA axis.

A limitation of our study is that it only included subjects without knee or motor control pathologies, and the mean angular differences reported therein may not generalise directly to populations with pathologies of the knee joint. Functional methods may require relatively large range of movement to be accurate. It may be difficult for patients with walking disabilities to perform such movement and the findings of this study, on an able-bodied population, may not translate directly to populations with restriction in their range of movement. It is however possible to assist patients with performing the functional calibration movement [33] and our results show that functional methods performed well with passive flexion-extension movements.

It is important to note that the range of the results exceeded 15° for all conventional and functional methods (Fig. 2), which indicate that these methods may provide inconsistent results. Hence, EOS biplanar radiographs or an alternative medical image based technology (e.g. 3D freehand ultrasound, [29]) may still be required when major surgical decision, such as derotational osteotomies, depend on the reliable orientation of the frontal plane of the femur and accurate hip rotation kinematics.

Conflict of interest statement

The authors declare they have no financial or personal relationships with other people or organization that could inappropriately influence their work.

Acknowledgment

The authors are grateful to Vicon Motion Systems (Oxford Metrics Group, UK) for the loan of the motion capture system necessary for the fulfillment of this study.

References

[1] J.R. Davids, S. Ounpuu, P.A. DeLuca, R.B. Davis 3rd, Optimization of walking ability of children with cerebral palsy, Instr. Course Lect. 53 (2004) 511–522.
[2] M.H. Schwartz, A. Rozumalski, T.F. Novacheck, Femoral derotational osteotomy: surgical indications and outcomes in children with cerebral palsy, Gait Posture 39 (2014) 778–783.
[3] J.L. McGinley, R. Baker, R. Wolfe, M.E. Morris, The reliability of three-dimensional kinematic gait measurements: a systematic review, Gait Posture 29 (2009) 360–369.
[4] G. Wu, S. Siegler, P. Allard, C. Kirtley, A. Leardini, D. Rosenbaum, et al., ISB recommendation on definitions of joint coordinate system of various joints for the reporting of human joint motion-part I: ankle, hip, and spine. International society of biomechanics, J. Biomech. 35 (2002) 543–548.
[5] A.G. Schache, R. Baker, L.W. Lamoreux, Defining the knee joint flexion-extension axis for purposes of quantitative gait analysis: an evaluation of methods, Gait Posture 24 (2006) 100–109.
[6] R. Davis, P. DeLuca, Clinical gait analysis: current methods and future directions, Human Motion Analysis: Current Applications and Future Directions, 1996. 17–42.
[7] R.M. Ehrig, W.R. Taylor, G.N. Duda, M.O. Heller, A survey of formal methods for determining functional joint axes, J. Biomech. 40 (2007) 2150–2157.
[8] R. Baker, L. Finney, J. Orr, A new approach to determine the hip rotation profile from clinical gait analysis data, Hum. Mov. Sci. 18 (1999) 655–667.
[9] V. Camomilla, A. Cereatti, G. Vannozzi, A. Cappozzo, An optimized protocol for hip joint centre determination using the functional method, J. Biomech. 39 (2006) 1096–1106.
[10] M. Roland, M.L. Hull, S.M. Howell, Validation of a new method for finding the rotational axes of the knee using both marker-based roentgen stereophotogrammetric analysis and 3D video-based motion analysis for kinematic measurements, J. Biomech. Eng. 133 (2011) 051003.
[11] M.H. Schwartz, A. Rozumalski, A new method for estimating joint parameters from motion data, J. Biomech. 38 (2005) 107–116.
[12] W.R. Taylor, E.I. Kornaropoulos, G.N. Duda, S. Kratzenstein, R.M. Ehrig, A. Arampatzis, et al., Repeatability and reproducibility of OSSCA, a functional approach for assessing the kinematics of the lower limb, Gait Posture 32 (2010) 231–236.
[13] J. Dubousset, G. Charpak, W. Skalli, J. Deguise, G. Kalifa, EOS: A new imaging system with low dose radiation in standing position for spine and bone & joint disorders, J. Musculoskelet. Res. 13 (2010) 1–12.
[14] H. Pillet, M. Sangeux, J. Hausselle, R. El Rachkidi, W. Skalli, A reference method for the evaluation of femoral head joint center location technique based on external markers, Gait Posture 39 (2014) 655–658.
[15] M. Sangeux, H. Pillet, W. Skalli, Which method of hip joint centre localisation should be used in gait analysis? Gait Posture 40 (2014) 20–25.
[16] Y. Chaibi, T. Cresson, B. Aubert, J. Hausselle, P. Neyret, O. Hauger, et al., Fast 3D reconstruction of the lower limb using a parametric model and statistical inferences and clinical measurements calculation from biplanar X-rays, Comput. Methods Biomech. Biomed. Eng. 15 (2012) 457–466.
[17] D.G. Eckhoff, J.M. Bach, V.M. Spitzer, K.D. Reinig, M.M. Bagur, T.H. Baldini, et al., Three-dimensional mechanics, kinematics, and morphology of the knee viewed in virtual reality, J. Bone Joint Surg. Am. 87 (Suppl. 2) (2005) 71–80.
[18] ISO 5725-2: Accuracy (trueness and precision) of measurement methods and results – Part 2: Basic method for the determination of repeatability and reproducibility of a standard measurement method. ISO 5725-2: Accuracy (trueness and precision) of measurement methods and results – Part 2: Basic method for the determination of repeatability and reproducibility of a standard measurement method 1994.
[19] I. Soderkvist, P.A. Wedin, Determining the movements of the skeleton using well-configured markers, J. Biomech. 26 (1993) 1473–1477.
[20] L. Chiari, U. Della Croce, A. Leardini, A. Cappozzo, Human movement analysis using stereophotogrammetry. Part 2: instrumental errors, Gait Posture 21 (2005) 197–211.
[21] L.Y. Chang, N.S. Pollard, Robust estimation of dominant axis of rotation, J. Biomech. 40 (2007) 2707–2715.
[22] G. Wu, P.R. Cavanagh, ISB recommandation for standardisation in the reporting of kinematic data, J. Biomech. 28 (1995) 1257–1261.
[23] A. Leardini, L. Chiari, U.D. Croce, A. Cappozzo, Human movement analysis using stereophotogrammetry part 3: Soft tissue artifact assessment and compensation, Gait Posture 21 (2005) 212–225.
[24] U. Della Croce, A. Leardini, L. Chiari, A. Cappozzo, Human movement analysis using stereophotogrammetry. Part 4: assessment of anatomical landmark misplacement and its effects on joint kinematics, Gait Posture 21 (2005) 226–237.
[25] D.L. Churchill, S.J. Incavo, C.C. Johnson, B.D. Beynnon, The transepicondylar axis approximates the optimal flexion axis of the knee, Clin. Orthop. Relat. Res. 356 (1998) 111–118.
[26] T. Asano, M. Akagi, T. Nakamura, The functional flexion-extension axis of the knee corresponds to the surgical epicondylar axis: in vivo analysis using a biplanar image-matching technique, J. Arthroplasty 20 (2005) 1060–1067.
[27] D. Eckhoff, C. Hogan, L. DiMatteo, M. Robinson, J. Bach, Difference between the epicondylar and cylindrical axis of the knee, Clin. Orthop. Relat. Res. 461 (2007) 238–244.
[28] U. della Croce, A. Cappozzo, D.C. Kerrigan, Pelvis and lower limb anatomical landmark calibration precision and its propagation to bone geometry and joint angles, Med. Biol. Eng. Comput. 37 (1999) 155–161.
[29] E. Passmore, M. Sangeux, Defining the medial-lateral axis of an anatomical femur coordinate system using freehand 3D ultrasound imaging, Gait Posture 45 (2016) 211–216.
[30] L. Blankevoort, R. Huiskes, A. de Lange, Helical axes of passive knee joint motions, J. Biomech. 23 (1990) 1219–1229.
[31] M.A. Freeman, V. Pinskerova, The movement of the normal tibio-femoral joint, J. Biomech. 38 (2005) 197–208.
[32] E.S. Grood, W.J. Suntay, A joint coordinate system for the clinical description of three-dimensional motions: application to the knee, J. Biomech. Eng. 105 (1983) 136–144.
[33] A. Peters, R. Baker, M.E. Morris, M. Sangeux, A comparison of hip joint centre localisation techniques with 3-DUS for clinical gait analysis in children with cerebral palsy, Gait Posture 36 (2012) 282–286.